

1 **An integrated geophysical and GIS based approach improves estimation of peatland**  
2 **carbon stocks.**

3

4 D. Carless<sup>1,2\*</sup>, B. Kulesa<sup>1</sup>, A. D. Booth<sup>1,3</sup>, Y. Drocourt<sup>1,4</sup>, P. Sinnadurai<sup>5</sup>,  
5 F. Alayne Street-Perrott<sup>1</sup>, P. Jansson<sup>6</sup>

6 <sup>1</sup> College of Science, Swansea University, Singleton Park, Swansea, SA2 8PP, UK

7 <sup>2\*</sup> Geography Department, University of Exeter, Rennes Drive, Exeter, Devon EX4 4RJ, UK

8 <sup>3</sup> Institute of Applied Geoscience, School of Earth and Environment, University of Leeds,  
9 Leeds, LS2 9JT, UK

10 <sup>4</sup> ACRI-ST, 260 Route du Pin Montard, BP 234, 06904 Sophia-Antipolis, France

11 <sup>5</sup> Brecon Beacons National Park Authority, Cambrian Way, Brecon LD3 7HP, UK

12 <sup>6</sup> Department of Physical Geography, Stockholm University, 106 91 Stockholm, Sweden.

13 \* Corresponding author: D.Carless@Exeter.ac.uk.

14 **Abstract:**

15 Estimations of peatland carbon stocks often use generalised values for peat thickness and  
16 carbon content. Ground penetrating radar (GPR), a rapid technique for field data  
17 collection, has been increasingly demonstrated as an appropriate method of mapping peat  
18 thickness. Light Detection and Ranging (LiDAR) data as a method for understanding  
19 peatland surface elevation are also becoming more widely available. Reliable mapping  
20 and quantification of site-specific carbon stocks (e.g. upland raised bogs) is therefore,  
21 becoming increasingly feasible, providing a valuable contribution to regional, national  
22 and potentially global carbon stock assessments. This is particularly important because  
23 raised bogs, such as those found in South Wales are considerable carbon stores. They are,  
24 however, susceptible to climate warming owing to their southerly location within the UK.  
25 Accurate estimates of peatland carbon stocks has broader importance because world-wide

26 peatland carbon stores are significant and threatened by climate change, posing a  
27 substantial challenge not only due to climate feedbacks if this stored carbon is released  
28 into the atmosphere, but also the impact on the other ecosystem services that they  
29 provide.

30

31 Here, we assess the value of an integrated GPR, LiDAR and Geographic Information  
32 System (GIS) approach to improve estimation of regional carbon stocks. We apply the  
33 approach to three ombrotrophic raised bogs in South Wales, UK, selected for their  
34 conservation value and their topographically-confined raised bog form.

35 GPR and LiDAR are found to be well suited, respectively, to mapping peat thickness at  
36 bog scale and surface elevation, thus allowing surface and basal topographies to be  
37 evaluated using GIS. In turn, this allows peat volumes to be estimated. For the first time,  
38 we record values between 55,200 m<sup>3</sup> and 163,000 m<sup>3</sup> for the sites considered here.

39 The greater confidence in these peat volume estimates results from the ability to calibrate  
40 the GPR velocity using a depth-to-target calibration with peat cores extracted at locations  
41 encompassing the deepest bog area. Peat thickness is mapped at the bog scale with near  
42 centimetre precision, improving the robustness of subsequent volume calculations and our  
43 understanding of the contribution of these small but numerous sites to regional carbon  
44 stocks. Our evaluation shows that GPR corresponds well with conventional manual  
45 probing but is minimally invasive and therefore less disturbing of sensitive peatland sites,  
46 while also offering improved coverage and spatial resolution with less time and cost.

47 In combination with measured bulk density and organic carbon contents, these peat  
48 volumes allow carbon stocks to be estimated with greater confidence compared to

49 conventional approaches, having values between 2,181 ±122 tonnes carbon and 6,305  
50 ±351 tonnes carbon at our three sites.

51 Keywords: ground-penetrating radar; peat; bog; carbon stock; LiDAR; GIS

## 52 **1. Introduction**

53 Terrestrial carbon stores are considerable. Peatlands in particular, whilst only covering ~3%  
54 of the earth's surface, account for approximately one third of all soil carbon storage (Gorham,  
55 1991; Yu et al., 2011). In the UK, peatlands in their various forms (blanket bog, raised bog  
56 and fens) account for almost 10% of the land area (approximately three million hectares) and  
57 store approximately 3.2 Gt of carbon (Bain et al., 2011). The UK BEIS Emissions Inventory  
58 for Peatlands project estimated that there are 90,000 ha of peatlands in Wales (Evans et al.,  
59 2017); however, roughly two thirds are thought to be in a degraded state.

60 Emissions from damaged peatlands are of global significance. Peatland landscapes that have  
61 been drained or experience fires are estimated to release 1.3 Gt of CO<sub>2</sub> annually, this  
62 contributes 10% of greenhouse gas emissions from the land use sector (IUCN, 2017) and  
63 constitutes a major part of national greenhouse gas emissions in many countries (Joosten et  
64 al., 2012). The Kyoto Protocol of 2008; an agreement within the United Nations' (UN)  
65 Framework Convention on Climate Change and the 2012 Doha Amendment, committed its  
66 parties to internationally binding greenhouse gas emission reduction targets (United Nations,  
67 2012). Accordingly, updated international carbon accounting rules mean that peatland soils,  
68 and specifically changes in carbon stocks as a result of activities related to wetland drainage  
69 and rewetting, can be voluntarily considered for reporting of CO<sub>2</sub> emissions (Blain and  
70 Murdiyarso, 2013).

71 In addition to emissions, peatland carbon losses can also occur as dissolved organic carbon  
72 and particulate organic carbon. Accurate assessment, including improved measuring,

73 reporting and verification of the global peat-carbon store is therefore necessary to support  
74 governmental inventories and also for the purpose of informing global climate change  
75 models, including for the prediction of potential positive climate feedbacks from degraded  
76 peatlands (Gallego-Sala et al., n.d.; Gorham, 1991)

77 Sustainable management and restoration of peatlands is one of the most cost-effective ways  
78 to mitigate climate change by reducing greenhouse gas emissions and minimizing carbon loss  
79 from peat soils (Joosten et al., 2012). In recognition of this, the Welsh Government has  
80 prioritised an ambitious programme to ensure that all peatlands supporting semi natural  
81 habitats are under active management by 2030 and are aiming for 95% of Wales' peatlands to  
82 be in 'good' condition by 2040 (Welsh Government, 2019a, 2019b, 2019c). Peatland  
83 restoration (involving the many techniques which aim to restore ecohydrological function  
84 such as blocking drainage ditches and sphagnum planting) is required in order to ensure the  
85 future resilience of these habitats and the ecosystem services they provide including; the  
86 provision of drinking water, surface water attenuation, carbon sequestration and storage, and  
87 the provision of a landscape of recreational and cultural value (Bain et al., 2011; Grand-  
88 Clement et al., 2013; Joosten and Clarke, 2002).

89 A significant challenge to peatland management and policy development, however, is that  
90 regional carbon estimates for peatlands are often lacking and can contain inaccuracies due to  
91 the inconsistent and wide ranging methodologies employed, as well as the sometimes  
92 inappropriate use of published estimates rather than physically measured data (Parry et al.,  
93 2012; Parsekian et al., 2012; Petrokofsky et al., 2012; Yu, 2012). For example, over the last  
94 50 years numerous estimates of UK peatland carbon storage have been published, ranging  
95 from around 3 Gt C to 7.8 Gt C (Billett et al., 2010; Bradley et al., 2005; Cannell et al., 1993;  
96 Lindsay, 2010; Milne and Brown, 1997). These inconsistent figures are largely a result of the  
97 different definitions of peat soils and methodologies used across the different regions of the

98 UK and the use of generalised estimates for peat thickness, bulk density and carbon content  
99 (Charman, 2002; Joosten and Clarke, 2002).

100 Carbon accounting in particular is further hampered by limited data on the key variables  
101 required for peatland carbon stock assessments, including fine-spatial scale mapping of  
102 peatland topography and accurate estimates of peat extent, thickness, peat bulk density and  
103 carbon content (Carless et al., 2019; Gatis et al., 2019). Historically, national carbon  
104 estimates for peat soils in the UK have been based on sparse field measurements and whilst  
105 studies such as Evans et al. (2016) provide data for these peat characteristics and carbon stock  
106 values for peat profiles from a Welsh site, it remains that detailed carbon stock assessments  
107 of Welsh peatlands are rare. Furthermore, the sites studied by Evans et al., (2016) were  
108 lowland fen (minerotrophic) sites and the applicability of these values to raised bog  
109 (ombrotrophic) sites, as investigated in this study, is limited due to differences in peat  
110 properties (e.g. bulk density) and ecohydrological functioning. The 2007 ECOSSE report  
111 (Smith et al., 2007) provides an estimation of the total carbon stored in peat and organo-  
112 mineral soils across Wales, being almost 0.2 Gt C. This was higher than any previous  
113 estimates (e.g. Bradley et al., 2005) due to the inclusion of peat greater than 1 metre in  
114 thickness, modifications to bulk density values (predicted using regression equations) and the  
115 methods used to calculate areas (soil map units). The inclusion of deeper peats was an  
116 important recognition that peat thickness can be extremely variable. Raised bogs (an Annex 1  
117 priority habitat listed in the EU Habitats Directive, (*European Commission, 2007*) for  
118 example, often develop in basins and can contain peats 4-10 m thick. Studies that previously  
119 only considered up to 1 metre peat thickness are therefore likely to have resulted in  
120 underestimations in carbon stock calculations (Holden and Connolly, 2011).

121 Understanding the carbon storage of organic soils is particularly important for South Wales  
122 as it is home to some of the most climatically marginal (southerly) and most vulnerable

123 ombrotrophic raised bogs in the UK, which have also suffered from excessive grazing  
124 pressure, fires and industrial pollution in the past. Accurate quantification of the extensive  
125 Welsh peatland carbon store is further required as it may be amongst the first to be affected  
126 by future climate warming (Gallego-Sala et al., 2010).

127

128 Only a small number of UK sites have been studied with the aim of quantifying carbon  
129 storage (Charman et al., 2013; Evans et al., 2016; Lindsay, 2010; Loisel et al., 2014; Ostle et  
130 al., 2009; Smith et al., 2007; Wellock et al., 2011). In this study, three raised bog sites in  
131 South Wales were assessed to (1) assist in alleviating the paucity of UK carbon stock  
132 estimates; (2) evaluate the scope of ground penetrating radar (GPR) measurements integrated  
133 with geographical information system (GIS) modelling in attaining peat thickness and  
134 volume estimates for the purpose of estimating peat carbon stocks; and (3) identify the  
135 suitability of this approach to regional upscaling of carbon stock estimates. This was achieved  
136 through the use of geophysical techniques (GPR) and remote sensing data (Light Detection  
137 and Ranging (LiDAR) Digital Terrain Model (DTM)). These datasets were integrated within  
138 a GIS (ArcGIS Pro) to extract peat volumes facilitating carbon stock estimates.

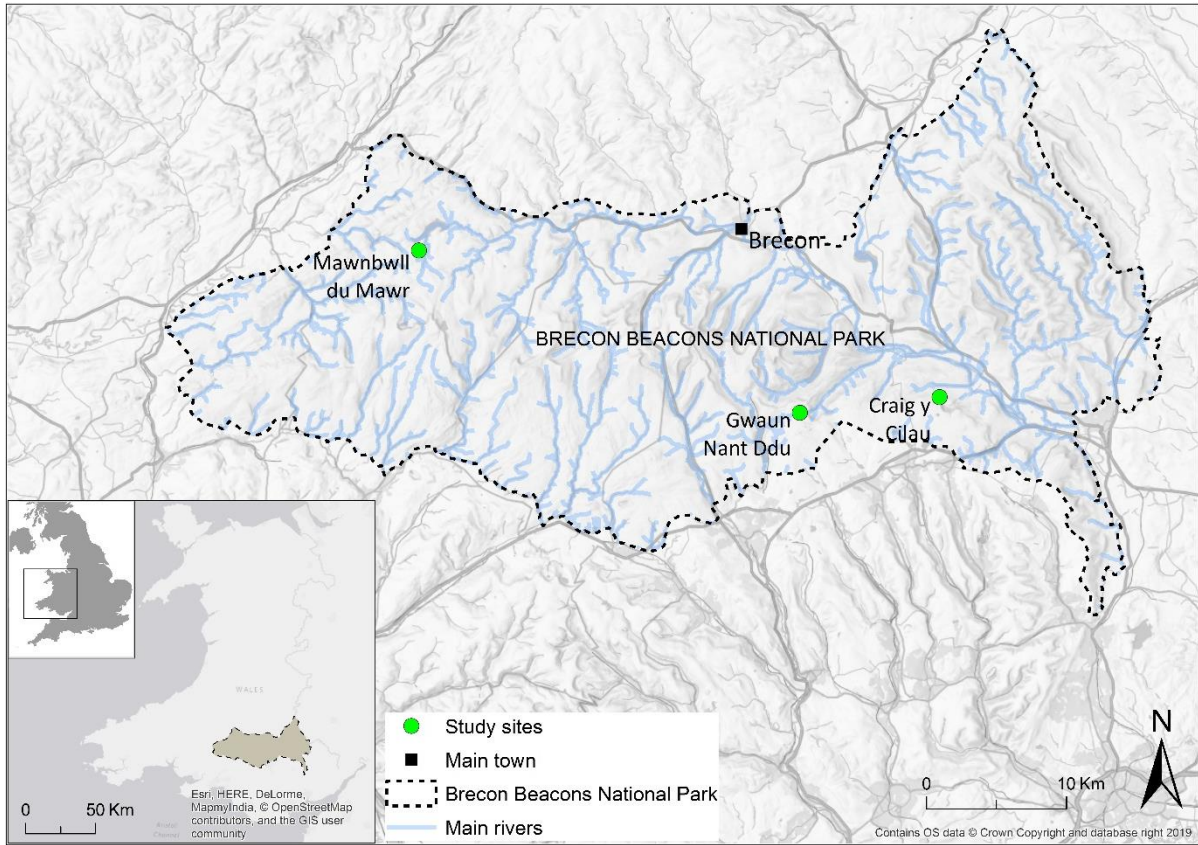
## 139 **2. Material and Methods**

### 140 **2.1. Research site locations**

141 The Brecon Beacons National Park, South Wales, hosts one of the most spectacular upland  
142 areas in Britain. The topography is varied with much of the park having an elevation over 300  
143 m a.s.l. The National Park experiences a maritime climate which is locally modified by  
144 altitude and topography with a recognised climatic gradient across the park from the west to  
145 the east, a distance of ~ 80 km. The average annual rainfall in the western extreme of the park  
146 is over 2400 mm, whilst in the east rainfall is only 1500 mm (George, 1990; Pratt-Heaton,  
147 1999). The geology of the park varies from north to south. The northern two thirds of the

148 park is underlain by Devonian Old Red Sandstone. In the southern sector, a thin band of  
149 (Dinantian) Carboniferous Limestone runs from west to east, separating the Old Red  
150 Sandstone uplands from the southern Namurian Basal Grits. The southern limit of the park is  
151 bounded by the northern edge of the South Wales coal measures formation.

152 Three raised bog sites totalling approximately 12 ha within the Brecon Beacons National  
153 Park were studied (Figure 1). The study sites were chosen because of their particular  
154 conservation value (Natura 2000 designated sites) or allocation for future improvements/  
155 restoration (e.g. New LIFE for Welsh raised bogs Project) as identified by the Brecon  
156 Beacons National Park Authority (BBNPA) and included 1) Mawnbwll du Mawr, 2) Gwaun  
157 Nant Ddu and 3) Waun Ddu bog within the Craig y Cilau National Nature Reserve (Figure  
158 1). Each are classified as an ombrotrophic raised bog, which have developed within  
159 topographically confined basins and exhibit typical features of lagg, rand and shallow domes.  
160 Surface vegetation is dominated by graminoid and Ericaceae species with expanses of  
161 sphagnum in wetter areas. All sites exhibit some degradation evidenced by areas of bare peat.



162

163 *Figure 1. Location of study sites within BBNP, and the location of the park within Wales and UK (inset maps).*

164

## 165 **2.2. Background to methodological approach**

166 Carbon stock estimates are most often achieved by calculating the carbon stored per unit  
 167 volume of peat. This requires accurate figures for peat spatial extent, peat thickness and  
 168 carbon density.

169 Peat spatial extent and thickness are most often approximated from aerial images or soil maps  
 170 (Cannell et al., 1999; Cruickshank et al., 1998; Milne and Brown, 1997), meaning that  
 171 regional averages for carbon stocks are based on limited physical sampling, or a generic peat  
 172 thickness, such as 1 m, is applied (Petrokofsky et al., 2012; Yu, 2012).

173 The most common techniques for the collection of measured peat thickness data include  
 174 coring, probing and digging trial pits. These point measurements are costly, being both time



175 and person intensive (Gatis et al., 2019; Jol and Smith, 1995; Proulx-McInnis et al., 2013).  
176 Authors have noted that peat thickness data from manual probing (inserting a thin metal rod  
177 into the peat until resistance is felt) can also be prone to uncertainties leading to considerable  
178 over- and underestimation. Uncertainties are explained as caveats for the methods including  
179 those associated with the obliquity of the probe and the strength and subjectivity of the probe  
180 operator in identifying the peat-mineral soil interface. If the mineral substrate beneath the  
181 peat is unconsolidated material (e.g. in peatlands formed by the terrestrialisation of a small  
182 waterbody), then the probe can penetrate the soft lake sediments (gyttja) and a depth beyond  
183 the base of the peat will be recorded. Measurements may also be affected by the presence of  
184 obstacles (e.g. buried wood) which prevent the probe reaching the base (Doolittle and Butnor,  
185 2009; Jol and Smith, 1995; Parry et al., 2014; Proulx-McInnis et al., 2013; Sass et al., 2010;  
186 Worsfold et al., 1986). Furthermore, these methods, which rely on interpolating between  
187 limited, manually-measured points may fail to capture sufficiently the fine-scale spatial  
188 variation in thickness, a result of variable underlying topography. Finally, being invasive  
189 methods they are unsuitable for many sensitive peatland sites, particularly if repeated  
190 assessments are required (Holden et al., 2002; Lindsay et al., 2014; McClellan et al., 2017;  
191 Parsekian et al., 2012; Plado et al., 2011).

192 In the 1980s, identifying the need to improve the speed and accuracy of peatland field survey,  
193 the Geological Survey of Finland investigated the use of GPR technology. The peat thickness  
194 data obtained was found to achieve greater detail than that gained by traditional means  
195 (drilling/coring methods) (Hänninen, 1992). Around the same time, Ulriksen (1982), also  
196 suggested that peat thickness from GPR were substantially more accurate than those achieved  
197 by drilling or probing (Jol and Smith, 1995). Since then, geophysical techniques (e.g. GPR, 2-  
198 D resistivity and electromagnetic induction) have increasingly been employed in peatland  
199 studies across Canada, Ireland, Finland, Sweden, Russia, the United Kingdom and the United

200 States. GPR is particularly effective and numerous peatland investigations have successfully  
201 employed it to gain detailed peat thickness data, as well as a greater understanding of peat  
202 volumes and internal stratigraphy (Doolittle and Butnor, 2009; Jol and Smith, 1995;  
203 McClellan et al., 2017; Parry et al., 2014, 2012; Parsekian et al., 2012; Ryazantsev and  
204 Mironov, 2018; Sass et al., 2010; Warner et al., 1990). Other studies have used GPR to assess  
205 gas accumulation and locate peat pipes (Comas et al., 2005; Holden et al., 2002; Sass et al.,  
206 2010).

207 GPR systems work by recording the two-way travel-time (TwTT) of electromagnetic (EM)  
208 waves. Specifically, the time it takes (in nanoseconds) for a pulse of electromagnetic energy,  
209 emitted from a transmitting antenna, to propagate into the subsurface and to be reflected back  
210 to a receiving antenna from a subsurface interface. Thickness is calculated by converting the  
211 measured TwTT to distance, using a known EM wave velocity. The velocity of the EM wave  
212 is directly dependent on relative dielectric permittivity ( $\epsilon_r$ ), a geophysical property strongly  
213 dependent on water content (Warner et al., 1990). The strength of the electromagnetic (EM)  
214 wave reflection depends on the contrast (reduction) in the volumetric moisture content  
215 between the peat and the underlying mineral soil. It is also dependant on the concentration of  
216 solutes in the pore water. Accordingly, GPR is generally more successful in investigations of  
217 ombrogenous peat (e.g. raised bogs and blanket peat) rather than minerogeneous (fen) sites  
218 because there are less inputs so a lower pH and basic cation content (Ca, Mg, Na, K) of pore  
219 water is found (Doolittle and Butnor, 2009; McClellan et al., 2017; Proulx-McInnis et al.,  
220 2013; Warner et al., 1990). Uncertainties in peat thickness achieved via the GPR method are  
221 attributable to the accuracy of the EM wave velocity used for the time-depth conversion and  
222 to the potential spatial variability in depth-integrated radar velocities. For example, some  
223 regions of the peatland might be drier than others and hence would likely have somewhat  
224 higher radar velocities than the overall wetter areas. Even where the peatland has comparable

225 wetness, pore waters maybe more concentrated in ionic contents in some regions than others,  
226 which would also cause local/regional-scale differences in peat thickness estimates. It is  
227 therefore recommended that where possible, site specific velocity calibrations are completed  
228 through depth-to-target calibration via manual survey or common midpoint survey (CMP)  
229 (Comas et al., 2005; Parry et al., 2014; Proulx-McInnis et al., 2013; Rosa et al., 2009).

230 Studies which have sought to compare GPR with probing or coring methods have confirmed  
231 that the technique produces accurate data sets (less subjective, higher vertical and horizontal  
232 resolution, higher data density). GPR surveying is typically rapid and provides a continuous  
233 sub-surface profile along the survey transect at a resolution unachievable by traditional  
234 methods (Doolittle and Butnor, 2009; Jol and Smith, 1995; McClellan et al., 2017; Parry et  
235 al., 2014; Parsekian et al., 2012; Proulx-McInnis et al., 2013).

236 Through geostatistical interpolation (e.g, the process of ordinary kriging) the GPR derived  
237 peat thickness data is gridded (2m x 2m) and subsurface topographies plotted. When  
238 calculated volumes are combined with estimates of peat carbon density, more robust  
239 estimates of total carbon stock can be achieved (Fyfe et al., 2014; Parsekian et al., 2012; Rosa  
240 et al., 2009).

241 Here we use a combination of GPR and LiDAR data to constrain GIS-based calculations of  
242 carbon stocks, as detailed in the following sections.

243

### 244 **2.3. Peat bog delineation**

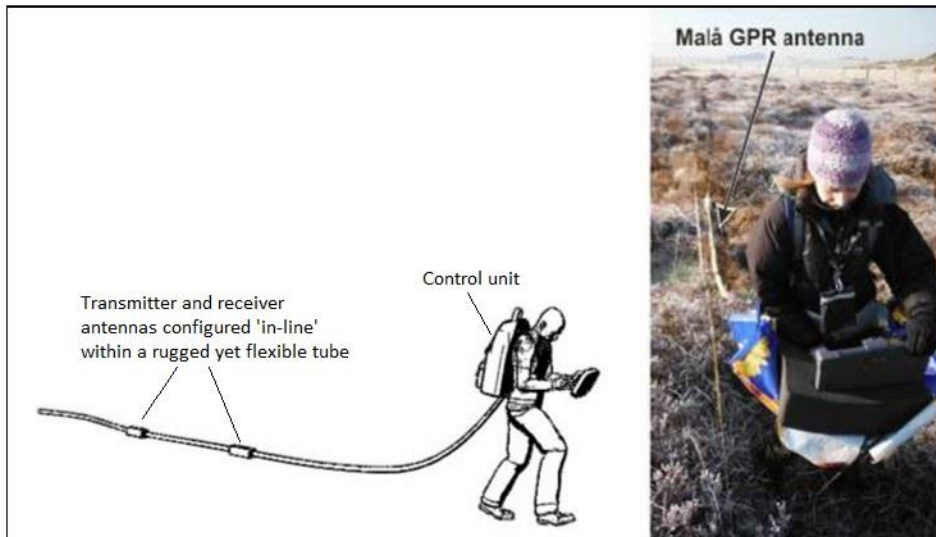
245 The lagg (stream) of a raised bog is the transition zone where runoff collects from the  
246 ombrotrophic (rain-fed) bog at its margin with the adjacent mineral soils (Howie and  
247 Meerveld, 2011). In this study, a combination of aerial images and LiDAR DTM data were  
248 analysed in ArcGIS. This allowed identification of the lagg stream at sites Gwaun Nant Ddu

249 and Craig y Cilau, which were subsequently digitised to create a bounding polygon. At site  
250 Mawnbwll du Mawr the hydrology is more complex and the lagg stream was not easy to  
251 define from the aerial imagery. The bog perimeter was therefore established by interpreting  
252 bog to non-bog vegetation changes in aerial images and confirmed on site. Digitised  
253 boundaries were further validated in the field and in interpretation of the base peat reflection  
254 in the GPR data to ensure that in all cases the area bounded by the polygon and subsequently  
255 used for peat thickness and volume extraction, included only peat with a minimum thickness  
256 of 0.3 m as required for classification as a peat soil (Joosten and Clarke, 2002; Lindsay,  
257 2010).

258

#### 259 **2.4. GPR surveying for peat thickness measurements**

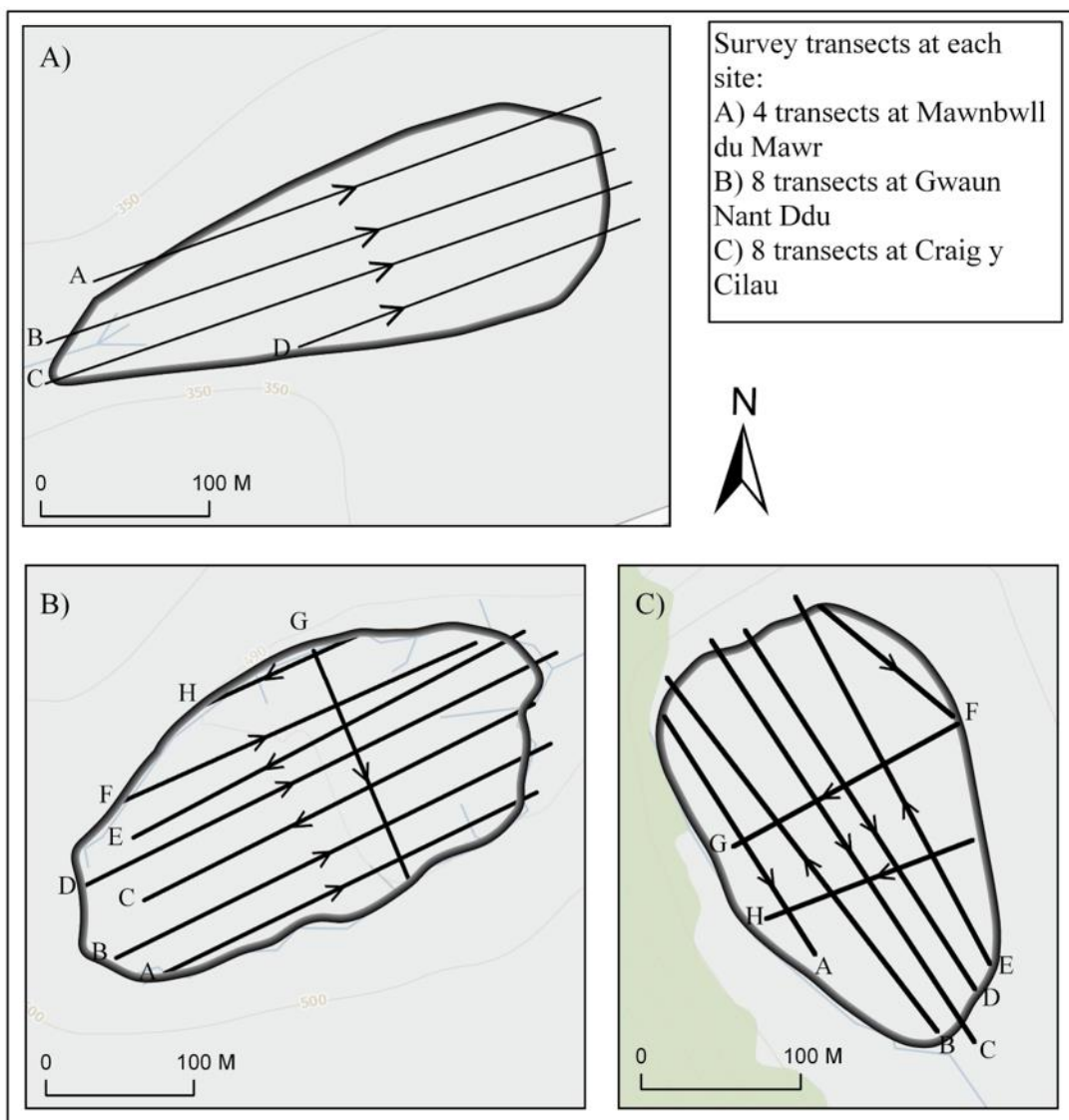
260 Peat thickness data for the three locations were collected by GPR survey. Data were acquired  
261 using a 100 MHz MALÅ Rough Terrain Antenna (RTA), an ‘in-line’ system involving a  
262 rugged, flexible cable, within which the transmitter and receiver electronics are separated by  
263 2 m (see Figure 2). A single user can tow the cable behind them as they walk along the  
264 survey transect. The advantage of the flexible cable system is that good ground contact can be  
265 maintained even on rough, vegetated surfaces (Francke, 2012) and the cable slides  
266 continuously through the vegetation with minimal disturbance to it or the bog surface.  
267 Furthermore, continuous, rapid and fine-scale sampling (<1m spacing, depending on walking  
268 speed) can be collected.



269

270 *Figure 2. Illustration of Malå Rough Terrain Antenna (adapted from Francke, 2012) and its use in the field.*

271 Over 5 km of GPR profiles were collected across the three sites. GPR survey transects  
 272 following the long axis of the bogs were pre-marked with tapes and start and finish points  
 273 logged in a handheld GPS (Garmin eTrex handheld unit) (Figure 3; Gwaun Nant Ddu and  
 274 Craig y Cilau also having cross-transect surveys for validation). In a GPR survey the  
 275 antennae are moved along the survey line (transect) and a series of traces (a record of the  
 276 measured EM wave reflection) are collected at specific points along the line. Successive,  
 277 multiple radar traces are taken at each sampling location which are automatically summed  
 278 and averaged to produce one composite trace, reducing noise and improving signal  
 279 coherence. The spacing between traces was 0.5 m (manually triggered) and 16 stacks were  
 280 used for each trace, providing the best compromise between data quality and acquisition  
 281 speed for our purposes. A window length of 500 ns was used, giving an expected sampling of  
 282 5-6 m for typical electromagnetic wave velocities of 0.0330-0.0385 m/ns through peat  
 283 (Comas et al., 2005; Parry et al., 2014; Parsekian et al., 2012; Proulx-McInnis et al., 2013;  
 284 Rosa et al., 2009; Sass et al., 2010).



Site	Transect length (m)							
	A	B	C	D	E	F	G	H
MDM	319	351.5	355	210	-	-	-	-
GND	280	330.5	333	350	300	276.5	185	132
CYC	182	275	300	298	260	129.5	175	145

286

287 *Figure 3. GPR survey transect orientation and lengths at sites A) Mawnbwll du Mawr (MDM), B) Gwaun Nant Ddu (GND)*  
 288 *and C) Craig y Cilau (CYC).*

289

290 GPR data processing was undertaken using ReflexW software (Sandeimer, 2013) and was  
 291 purposefully limited to application of a time-zero correction, a “dewow” filter and bandpass  
 292 frequency filter. This sequence minimised processing artefacts while allowing a reflection to  
 293 be identified in all GPR profiles (Figure 5), interpreted as the interface between the peat and

294 the mineral soil. Although generally prominent, the reflection's signal-to-noise ratio is  
295 somewhat degraded in the deepest regions of the bogs; signal attenuation may have been  
296 enhanced owing to a basal layer of electrically conductive limnic clay, and in small sections  
297 by in-wash of more mineral sediments at the edges of the bogs. Consequently, with the  
298 exception of some short sections of transects on Gwaun Nant Ddu and Craig y Cilau, the  
299 onset of the basal reflection could be manually picked throughout the data volume, with a  
300 typical precision of  $\pm 1.5$  ns (Gusmeroli et al., 2012).

301

302 Peat thickness was also evaluated using a manual probe at 74 locations (Mawnbwll du Mawr  
303 = 17, Gwaun Nant Ddu = 26, Craig y Cilau = 31), both to infill small gaps in the radar  
304 coverage (e.g., as a result of signal attenuation) and to provide initial calibration of GPR  
305 velocity estimates for conversion of TwTTs to peat thicknesses. Manual probing was  
306 completed following the standard method of inserting rods until resistance is felt. Resistance  
307 is assumed to be the peat-mineral interface with the depth at which this is encountered being  
308 recorded as the peat thickness (Parsekian et al. 2012). The location of each measurement  
309 point was recorded with a hand-held GPS. Assuming that the probe had reached the base of  
310 the peat, comparing the measured thickness to the TwTT in the GPR profiles data implied a  
311 preliminary radar velocity of 0.0343 m/ns, later refined following comparison to core data  
312 (see next section). An independent estimate of GPR velocity using, e.g., common midpoint  
313 survey methods (Huisman et al., 2003) was not possible in this study, given the fixed offset  
314 between the transmitter and receiver in the RTA system.

315

## 316 **2.5. Peat core selection, sampling and analysis**

317 The thickest peat sections at each site were identified from our radargrams, allowing targeted  
318 core sampling. A master core was extracted from each site for laboratory analysis of bulk

319 density and carbon content. Using a Livingstone piston corer with a 5 cm diameter, stainless  
320 steel barrel, cores representing the total peat thickness were recovered from Gwaun Nant Ddu  
321 and Craig y Cilau sites. At Mawnbwll du Mawr, however, the core failed to achieve the full  
322 known thickness of peat due to resistant layers which could not be penetrated despite multiple  
323 efforts.

324 For peat analysis, cores were sampled at 4 cm resolution and bulk density estimated from  
325 subsamples of known volume, dried at 105 °C. Loss-on-ignition was calculated for every  
326 subsample using standard methods (Chambers et al., 2011) to estimate percentage organic  
327 matter content, and calibrated by direct measurement (via elemental analysis) of total organic  
328 carbon of a selection of samples (n=116).

329

330 In addition to providing material for bulk density and carbon analyses, LOI analysis of the  
331 core identified the depth at which the peat - mineral soil interface occurred, facilitating  
332 improved velocity calibration for the depth conversion of base-peat travel-times identified in  
333 the GPR data. The calibrated GPR velocity is  $0.0352 \pm 0.0005$  m/ns based on the two study  
334 sites at which the full thickness of peat was achieved, where  $\pm 0.0005$  m/ns is the standard  
335 error resulting from our assumption of a 5 cm nominal ambiguity in identifying a sharp  
336 contact at the transition from organic peat to limnic clay. This represents a ~2.5% increase  
337 over the initial velocity estimated from the probing (0.0343 m/ns) (see section 2.4) and lies  
338 squarely within the range of typical GPR velocities for peat (0.0330-0.0385 m/ns) (Proulx-  
339 McInnis et al., 2013; Rosa et al., 2009; Theimer et al., 1994). This velocity ( $0.0352 \pm 0.0005$   
340 m/ns) was therefore taken as the calibrated ground-truth throughout all subsequent volumetric  
341 assessments.

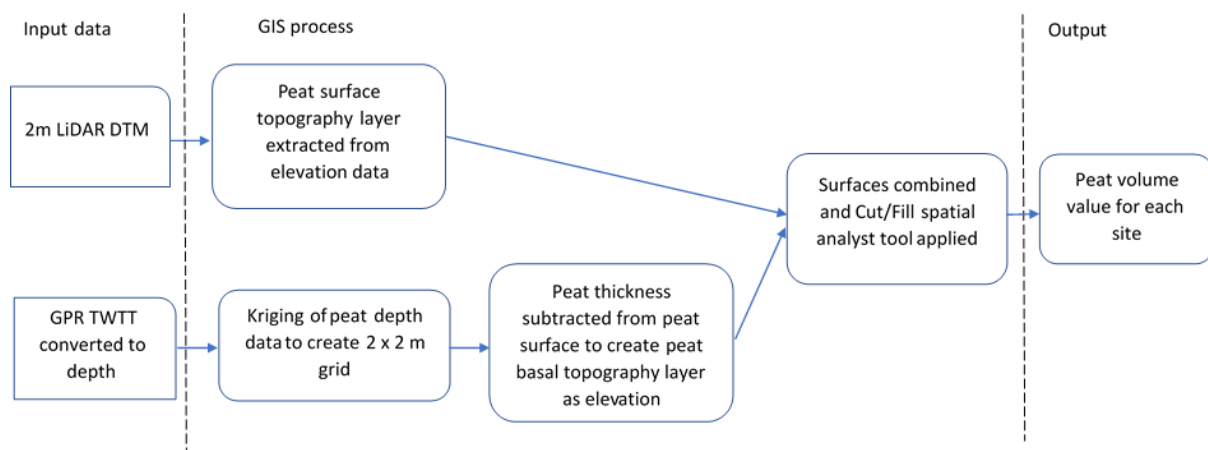
342

343 **2.6. Peat thickness mapping and calculation of peat volumes in GIS**



344 The 2m resolution LiDAR composite data from aerial surveys flown in November 2012 were  
 345 provided free of charge under a non-commercial use licence, by the Geomatics Group  
 346 (Environment Agency, 2013). Data pre-processed into Digital Terrain Models (DTM) were  
 347 provided in 1 km<sup>2</sup> tiles with an average vertical accuracy of ±15 cm and average horizontal  
 348 accuracy of ±40 cm.

349 Using a three-step workflow in ArcGIS (Figure 4), LiDAR DTM and GPR data were used to  
 350 generate (i) a peat surface topography layer, by extracting relevant surface elevation data (m  
 351 above sea level) from the DTM data; (ii) a peat basal topography layer, by interpolating peat  
 352 thicknesses (established from our GPR data) to a 2 x 2 m grid using the Kriging Geostatistical  
 353 Analysis tool in ArcGIS (Dallaire and Garneau, 2008; Goovaerts, 1997; Zeng and Huang,  
 354 2007) and subtracting the values from the peat surface layer (i) to produce a basal topography  
 355 layer as elevation (m above sea level); and (iii) a peat volume estimate by subtracting peat  
 356 basal topography from surface topography using the ArcGIS Cut/Fill tool (Price, 2002). This  
 357 was repeated for each of the three sites.



358  
 359 *Figure 4: 3-step workflow in GIS to achieve peat volume calculations*

360  
 361 **2.7. Estimation of carbon stocks**

362 As figures for the total volume of peat in a peatland site are relatively rare, calculations of  
 363 carbon stocks often ignore this parameter, preferring to calculate a carbon per unit volume

364 (e.g. per m<sup>3</sup>) and multiplying this by area and thickness (often limited to 1 m). In this study  
 365 however, LiDAR and GPR data were combined to model the peat basin volume. It was  
 366 therefore possible to calculate carbon stocks from the mass of organic matter within each site.  
 367 The mass of organic matter (kg) was established from peat volume (m<sup>3</sup>) and bulk density (g  
 368 cm<sup>3</sup>), using equation (1):

$$369 \quad \text{Mass}_{om} = V_i \times \rho_i \quad (1)$$

370 Where  $\text{Mass}_{om}$  is the mass of organic matter (peat);  $V_i$  is the volume of peat for site  $i$  and  $\rho_i$  is  
 371 the measured bulk density for the site.

372 Carbon stock ( $C_{stock}$ ) (kg C) for each site is then calculated from the product of the organic  
 373 matter mass ( $\text{Mass}_{om}$ ) and the fraction of organic matter that is carbon ( $OM_c$ ) established  
 374 from the calibrated LOI data, following equation (2):

$$375 \quad C_{stock} = \text{Mass}_{om} \times OM_c \quad (2)$$

376

## 377 **2.8. Explanation of estimation of uncertainties**

378 In order to estimate the uncertainty in the calculation of carbon stock, the method of error  
 379 propagation for multiplication of measured properties was applied (Bevington and Robinson,  
 380 2003). The uncertainties in the measured variables; volume (m<sup>3</sup>) (calculated using the  $\pm$   
 381 0.0005 m/ns standard error in depth) and density (g cm<sup>3</sup>) were carried over to determine the  
 382 uncertainty in the dependent variable; mass (kg).

383 To establish the effect that the uncertainties in both volume and density have on the  
 384 calculated mass, the following equation (3) is applied:

$$385 \quad \delta m = M \times \sqrt{\left(\frac{\delta v}{V}\right)^2 + \left(\frac{\delta d}{D}\right)^2} \quad (3)$$

386 Where,  $M$  is mass;  $V$  is volume;  $D$  is density;  $\delta m$  is the uncertainty in mass;  $\delta v$  is the  
 387 uncertainty ( $\pm 1\sigma$ ) in volume and  $\delta d$  is the uncertainty ( $\pm 1\sigma$ ) in density. The uncertainty in the

388 peat mass ( $\delta m$ ) is then carried through and combined with the uncertainty in the  
389 measurement of organic carbon in order to present an error estimate for the site specific  
390 carbon stock value.

391

### 392 **3. Results and discussion**

#### 393 **3.1. Geophysical results - peat thickness**

394 Basin depth, and therefore peat thickness, was found to vary both within and between sites. A  
395 summary of the maximum and mean depth to the peat-mineral soil interface recorded for  
396 each site are reported in Table 1. The maximum thickness of peat was 5.48 m, recorded at  
397 Gwaun Nant Ddu.

398 *Table 1 Maximum and mean peat thickness recorded, assuming a GPR velocity of 0.0352 m/ns.*

Site	Area (ha)	Max thickness (m)	Mean thickness (m)
Mawnbwll du Mawr	3.0	3.91	1.81
Gwaun Nant Ddu	4.8	5.48	3.41
Craig Y Cilau	3.8	5.39	2.66

399

400 The shallowest mean peat thickness was measured at Mawnbwll du Mawr. Here, the peat  
401 surface showed a subtle raised or domed area, as often seen with well-developed  
402 ombrotrophic bogs. The raised area was not central however, instead located in the  
403 northwestern region of the bog (Figure 7). Analysis of the GPR depth data confirmed that the  
404 dome was located above a shallow basal depression where the thickest peat was recorded.  
405 Gwaun Nant Ddu demonstrated a more typical raised bog profile, with an obvious and well-  
406 defined lagg, rand and dome. The GPR data illustrated that the peat had developed in a  
407 topographically confined hollow with the dome located relatively centrally over it. Peat  
408 thicknesses were highly variable and some of the thickest of all sites were recorded here.

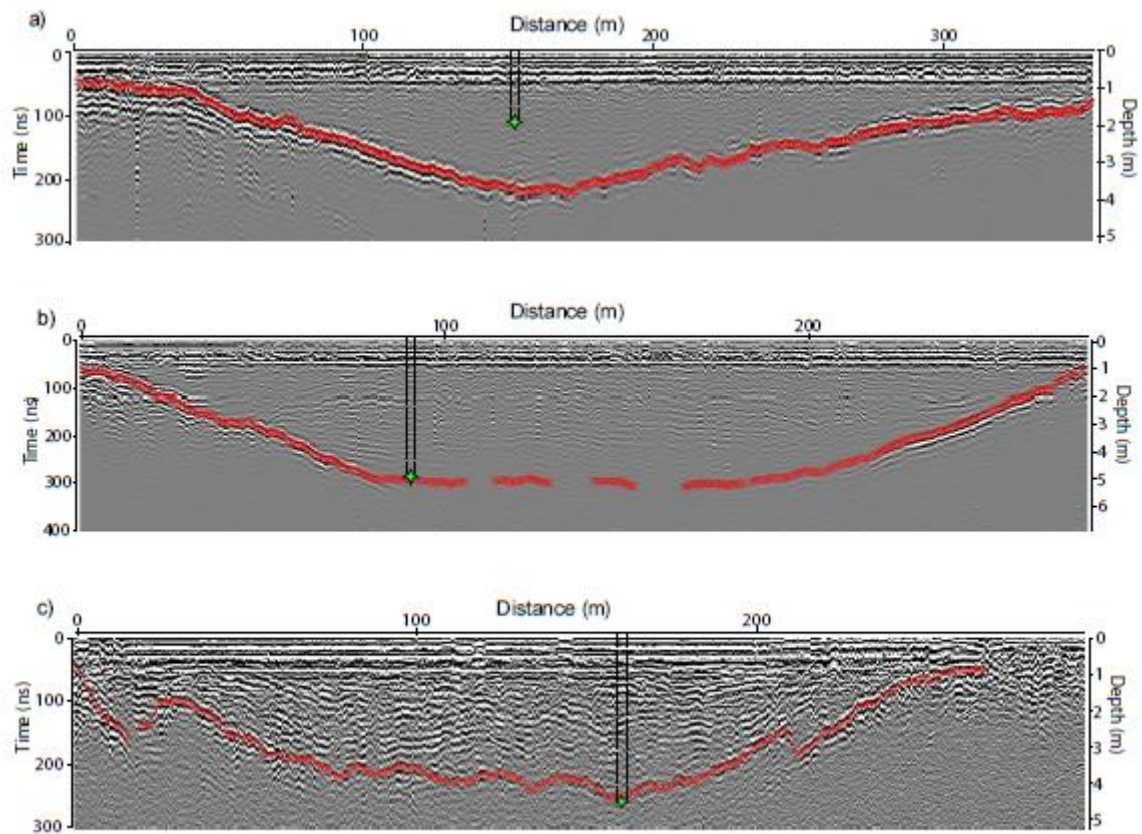
409 The GPR data from Craig y Cilau exhibited considerable small-scale variation in basal  
410 topography, illustrated by undulations in the basal reflection. A possible explanation for this  
411 is debris and boulders from the limestone escarpment which bounds its northern and western  
412 edges, falling into the basin prior to peat formation. Even so, a depression was recorded in the  
413 basal topography and a distinct dome formed the surface, confirmed by achieving greatest  
414 peat thickness measurements in this location.

### 415 **3.2. Validation of peat thickness from GPR using peat core data**

416 At Gwaun Nant Ddu and Craig Y Cilau, cores of 489 cm and 444 cm length were collected,  
417 respectively. The measured depth of peat from these two cores were found to be close to the  
418 peat depths measured by the GPR (Figure 5) and suggests that the assumption of using the  
419 same GPR velocity for both sites is acceptable.

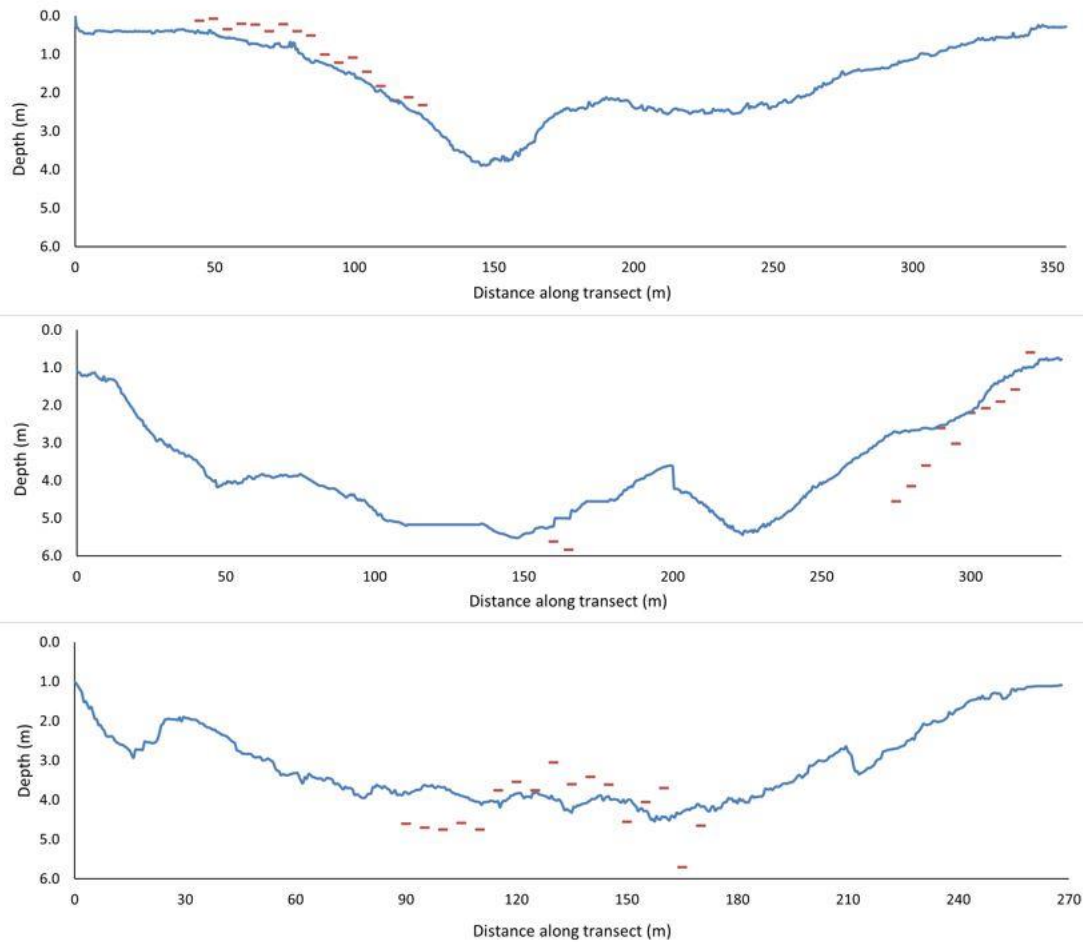
420 Additionally, a comparison of the GPR data with the loss-on-ignition data from peat core  
421 analysis gave further confidence that GPR is effective at recording the base of peat. At both  
422 these sites the coring had sampled fully the ombrotrophic peat and extended into the  
423 underlying mineral layer of the bog. This is evidenced by a significant drop in % organic  
424 matter in the LOI data. Accordingly, the depth at which a strong reflection was recorded in  
425 the radargram was shown to correspond well with the depth at which an increase in the  
426 mineral content of the peat was seen.

427 We were able to conclude therefore that GPR provides an appropriate method for identifying  
428 the base of the peat and the location of the greatest thickness of peat for core extraction.



429 *Figure 5. Location and depth of peat core plotted against radargram for a) Mawnbwll du Mawr, b) Gwaun Nant Ddu and c)*  
 430 *Craig y Cilau.*

431 Peat thicknesses from manual probing and GPR correlated well with each other (N=74, r-  
 432 value = 0.85, p value = <0.001). Notwithstanding, manual probing was found to both over-  
 433 and underestimate peat depths, when compared to GPR (Figure 6), likely due to difficulties  
 434 identifying the peat-mineral boundary and being subjective to the probe user. Manual probing  
 435 is also time consuming in achieving large sample sizes (for example to complete sampling at  
 436 high spatial resolution (0.5 m – 1 m spacing) along multiple 100+ m transects), compared to  
 437 GPR.

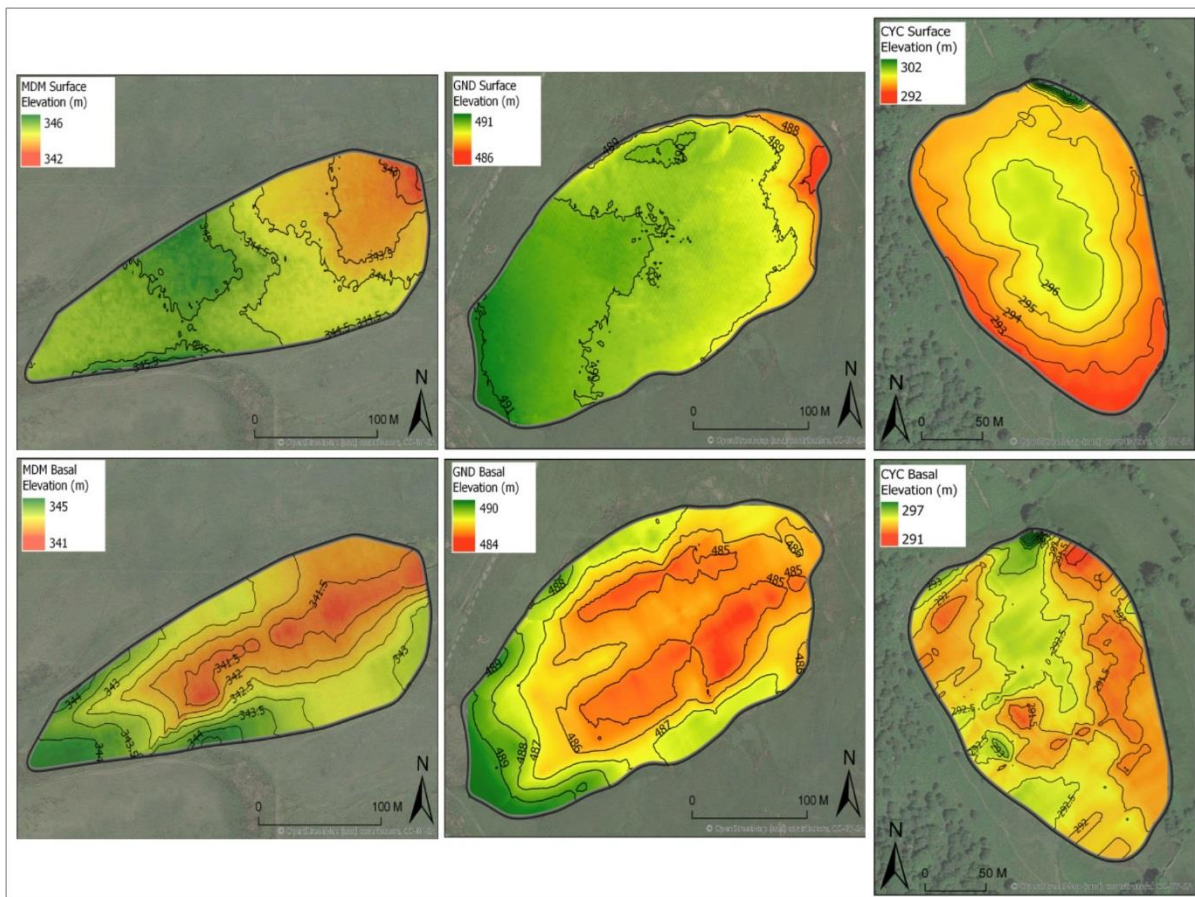


438

439 *Figure 6. Comparison of probing depths (red dashes) plotted against GPR peat base depths (blue line) for selected GPR*  
 440 *transects. A) Mawnbwl du Mawr, Line 3, B) Gwaun Nant Ddu Line 2 and C) Craig y Cilau Line 4. Note the different vertical*  
 441 *scales in the panes.*

442 **3.3. Peat thickness maps (kriging) and calculation of peat volumes in GIS**

443 Figure 7 shows contour plots of peat thickness at each site, subsequently used to evaluate  
 444 volumes (Table 2). The peat volume was calculated by converting GPR TwTT to thickness  
 445 using a velocity of  $0.0352 \pm 0.0005$  m/ns. The volume of Gwaun Nant Ddu bog is estimated  
 446 at  $163,000 (\pm 2285) \text{ m}^3$ , with Mawnbwl du Mawr and Craig y Cilau showing smaller volumes  
 447 of  $55,000 (\pm 773) \text{ m}^3$  and  $101,000 (\pm 1411) \text{ m}^3$ , respectively.



448

449 *Figure 7. Example surface elevation contour maps (Upper images) and sub-surface elevation contour map (Lower images)*  
 450 *for sites A) Mawnbwll du Mawr, B) Gwaun Nant Ddu and C) Craig y Cilau. Background image: Google Maps Hybrid.*

451

### 452 **3.4. Laboratory analysis – bulk density and carbon content**

453 Bulk density and total organic carbon are presented in Table 2. Our measured mean bulk  
 454 densities ( $\sim 0.07 - 0.08 \text{ g cm}^{-3}$ ) are within the range reported for ombrotrophic peats of  
 455 northern peatlands ( $0.07 - 0.15 \text{ g cm}^{-3}$ , Lindsay, 2010). They also compare well to figures  
 456 presented for basin peat  $>1\text{m}$  in Scotland ( $0.09 \text{ g cm}^{-3}$ , Chapman et al., 2009; Milne and  
 457 Brown, 1997) and a Welsh upland site ( $0.08 \text{ g cm}^{-3}$  at Plynlimon-Hafren, Smith et al., 2007).  
 458 Measured values for organic carbon content at our sites ( $\sim 51.0 - 51.5\%$ ) are towards the  
 459 upper end of typical values for northern peatlands ( $47 \pm 6\%$ , Loisel et al., 2014) and within  
 460 the range quoted for basin peats in Scotland ( $48.6 \pm 1.1 \%$  for  $0.3 - 1 \text{ m}$  peat depths and  $60.8$   
 461  $\pm 3.4 \%$  for  $>1 \text{ m}$  peat depths, Chapman et al., 2009).

462 **3.5. Carbon stock estimation**

463 Site Gwaun Nant Ddu returned the largest total peat (organic matter) mass with 12,200  
 464 tonnes which, when converted using carbon content, was calculated to represent a total  
 465 carbon stock of 6310 tonnes of carbon. Craig y Cilau was calculated to contain 8,070 tonnes  
 466 of organic matter, equating to a mean carbon stock of 4,110 tonnes of carbon. The smallest  
 467 site of the study, Mawnbwl Du Mawr, had an organic matter mass of 4,250 tonnes,  
 468 equivalent to 2,180 tonnes of carbon.

469 *Table 2. Summary table of peat analysis for each site – bulk density (g cm<sup>-3</sup>), organic matter (%), carbon content (%) and*  
 470 *carbon density (g C cm<sup>-3</sup>) and calculated peat volume (m<sup>3</sup>) and carbon stocks (t C). Values in parenthesis are standard errors*  
 471 *for all but Carbon Stock which are errors based on propagation of uncertainty (see section 2.8).*

	Bulk Density g cm <sup>-3</sup>	Mean organic content (%)	Mean carbon content (%)	Mean carbon density (g C cm <sup>-3</sup> )	Mean peat volume (m <sup>3</sup> )	Peat mass (t)	Carbon stock (t C)
Mawnbwl Du Mawr	0.077 (±0.002)	97.8 (±0.220)	51.3 (±0.210)	0.04 (±0.001)	55,202	4,250	2180 (±122)
Gwaun Nant Ddu	0.074 (±0.001)	96.5 (±0.347)	51.5 (±0.160)	0.04 (±0.001)	163,249	12,200	6310 (±351)
Craig y Cilau	0.080 (±0.001)	96.1 (±0.302)	51.0 (±0.131)	0.04 (±0.001)	100,811	8,070	4110 (±231)

472

473 **4. Discussion and conclusions**

474 We have demonstrated that combining peat thickness data from GPR survey and surface  
 475 elevation data from LiDAR in a GIS can improve characterisation of peatland sites and peat  
 476 volumes and therefore carbon stock estimations in a UK region that may respond particularly  
 477 rapidly to climate warming. GPR has at least three critical advantages compared to more  
 478 conventional manual probing in that it is (i) non-invasive and thus avoids disturbing the  
 479 sensitive bog vegetation or peat surface; (ii) rapid so that entire bogs can be surveyed in a  
 480 fraction of the time required for probing at the bog scale; and (iii) relatively reliable in  
 481 mapping peat thickness as a continuous lateral reflection across the sites, facilitating peat-  
 482 volume estimates with lower uncertainty than those calculated from lower spatial resolution



483 data interpolated from probing measurements, which are known to both over- and  
484 underestimate peat thickness.

485 GPR data analysis identified the thickest areas of peat from which cores were subsequently  
486 extracted. Laboratory analysis of the peat cores (LOI) allowed accurate identification of the  
487 depth of the peat-mineral soil interface, which served to ground-truth the base-peat GPR  
488 reflection. The radar propagation velocity through peat was subsequently calibrated, yielding  
489 a value of  $0.0352 \pm 0.0005 \text{ m ns}^{-1}$  that falls squarely within the cumulative velocity range  
490 reported in other extensive, worldwide peatland studies (Comas et al., 2005; Parry et al.,  
491 2012; Parsekian et al., 2012; Proulx-McInnis et al., 2013; Sass et al., 2010; Theimer et al.,  
492 1994). Once calibrated, GPR surveying facilitates peat thickness mapping with centimetre-  
493 scale precision (McClellan et al., 2017; Parry et al., 2014; Theimer et al., 1994).

494 GPR-derived peat thicknesses facilitated kriging of peat basal surfaces in GIS. These basal  
495 surfaces were then combined with a surface topography layer (LiDAR DTM) in ArcGIS to  
496 extract a peat volume, using the Cut/Fill analysis tool. This provided a uniquely detailed  
497 picture of peat basin morphology and volume of peat for these sites, from which we can  
498 calculate carbon content.

499 Bulk density and organic carbon content analyses were carried out for all three sites reported  
500 here, respectively yielding values of  $\sim 0.074 - 0.080 \text{ g cm}^3$  and  $\sim 51.0 - 51.5\%$  that agree  
501 with other published data for UK peatlands (Chapman et al., 2009; Charman et al., 2013;  
502 Lindsay, 2010; Loisel et al., 2014; Smith et al., 2007; Wellock et al., 2011).

503 The overall carbon stock values for our three sites were calculated from the volume estimates  
504 and carbon analysis, yielding values of  $6,310 \pm 351 \text{ t C}$  for Gwaun Nant Ddu,  $4,110 \pm 231 \text{ t C}$   
505 for Craig y Cilau and  $2,180 \pm 122 \text{ t C}$  for Mawnbwll du Mawr.

506

507 It is suggested that this novel combination of techniques could facilitate investigations of  
508 ombrogenous peatland sites, such as raised bogs or blanket peatlands, previously overlooked  
509 but which contain significant stocks of carbon when considered across wider regions. These  
510 sites are often sensitive and the subject of management plans but demonstrate degraded  
511 conditions. It is understood that healthy, actively peat-forming habitats function as carbon  
512 sinks, sequestering CO<sub>2</sub> via photosynthesis and due to limited decomposition of organic  
513 matter, transfer it into the soil carbon pool (Lal, 2008). Functioning peatlands can have a net  
514 long-term ‘cooling’ effect on the climate (Limpens et al., 2008; Yu et al., 2011). Accordingly,  
515 peatlands are increasingly recognised for their importance in the global carbon cycle and due  
516 to becoming ever more threatened ecosystems. Our findings have provided a better  
517 understanding of carbon stored in specific sites and their contribution to national carbon  
518 stocks. This could provide additional knowledge for national management strategies and for  
519 safeguarding against future carbon losses to the atmosphere.

520 In conclusion, peat thickness, volume and carbon stocks have been modelled to a new level  
521 of detail useful for regional planning and management of these sensitive sites. Our new  
522 approach could be widely adopted to allow inclusion of raised bogs in regional scale peat  
523 carbon stock assessments. We recognise that the use of GPR may incur costs for purchase or  
524 rental of equipment, but these are outweighed by the potential reduction in costs from savings  
525 in time and person hours for detailed surveys. Furthermore, the increasing availability of 1m  
526 spatial resolution LiDAR data (through the UK Environment Agency National LIDAR  
527 Programme), for mapping of peat bogs and free, open-source GIS software mean this  
528 methodology can easily be applied to other UK sites. Many European countries also now  
529 have LiDAR DTMs openly available (e.g. Estonia, Finland, Norway, Sweden). However, in  
530 areas where LIDAR data is not available, we suggest that GNSS receivers in conjunction  
531 with the GPR survey (i.e. mount a roving GNSS antenna on the radar system and then post-

532 process those data relative to a base station), could provide surface elevation data of equally  
533 adequate vertical and planimetric precision. GNSS instruments are widely available on a  
534 global scale and hence this approach should almost always be feasible. In the rare case that it  
535 is not possible then a constant topographic value (e.g. 0 m) could be assigned to the peat  
536 surface but it must be borne in mind that this would only be appropriate for peat deposits with  
537 a flat surface topography at the survey site scale and will give a less accurate estimate of peat  
538 thickness and associated volumes.

539

540

541 Acknowledgements:

542 The authors are grateful to the Brecon Beacons National Park Authority and Natural  
543 Resources Wales who granted access to sites. We would also like to thank Professor Siwan  
544 Davies, for co-supervision of the PhD from which this work has developed and to those who  
545 assisted with fieldwork.

546 This research was funded by KESS (Knowledge Economy Skills Scholarships) which is  
547 supported by the European Social Fund through the Welsh Government.

548 **References**

- 549 Bain, C.G., Bonn, A., Stoneman, R., Chapman, S., Coupar, A., Evans, M., Gearey, B.,  
550 Howat, M., Joosten, H., Keenleyside, C., Labadz, J., Lindsay, R., Littlewood, N., Lunt,  
551 P., Miller, C.J., Moxey, A., Orr, H., Reed, M., Smith, P., Swales, V., Thompson,  
552 D.B.A., Thompson, P.S., Van de Noort, R., Wilson, J.D., Worrall, F., 2011. IUCN UK  
553 Commission of Inquiry on Peatlands. IUCN UK Peatland Programme.
- 554 Bevington, P.R., Robinson, D.K., 2003. Data Reduction and Error Analysis for the Physical  
555 Science. McGraw-Hill, New York. Scientific Research Publishing.
- 556 Billett, M., Charman, D., Clark, J., Evans, C., Evans, M., Ostle, N., Worrall, F., Burden, A.,  
557 Dinsmore, K., Jones, T., McNamara, N., Parry, L., Rowson, J., Rose, R., 2010. Carbon  
558 balance of UK peatlands: current state of knowledge and future research challenges.  
559 *Clim. Res.* 45, 13–29. <https://doi.org/10.3354/cr00903>
- 560 Blain, D., Murdiyarso, D., 2013. Rewetted Organic Soils, in: Leifeld, J., Sanz Sanchez, M.J.  
561 (Eds.), 2013 Supplement to the 2006 IPCC Guidelines for National Greenhouse Gas  
562 Inventories: Wetlands. Intergovernmental Panel on Climate Change, Switzerland, pp. 1–  
563 42.
- 564 Bradley, R.I., Milne, R., Bell, J., Lilly, A., Jordan, C., Higgins, A., 2005. A soil carbon and  
565 land use database for the United Kingdom. *Soil Use Manag.* 21, 363–369.  
566 <https://doi.org/10.1079/SUM2005351>
- 567 Cannell, M.G.R., Dewar, R.C., Pyatt, D.G., 1993. Conifer plantations on drained peatlands in  
568 Britain: A net gain or loss of carbon? *Forestry* 66, 353–369.  
569 <https://doi.org/10.1093/forestry/66.4.353>
- 570 Cannell, M.G.R., Milne, R., Hargreaves, K.J., Brown, T.A.W., Cruickshank, M.M., Bradley,  
571 R.I., Spencer, T., Hope, D., Billett, M.F., Adger, W.N., Subak, S., 1999. National

572 inventories of terrestrial carbon sources and sinks: The U.K. Experience. *Clim. Change*  
573 42, 505–530. <https://doi.org/10.1023/A:1005425807434>

574 Carless, D., Luscombe, D.J., Gatis, N., Anderson, K., Brazier, R.E., 2019. Mapping  
575 landscape-scale peatland degradation using airborne lidar and multispectral data.  
576 *Landsc. Ecol.* 34, 1329–1345. <https://doi.org/10.1007/s10980-019-00844-5>

577 Chambers, F.M., Beilman, D.W., Yu, Z., 2011. Methods for determining peat humification  
578 and for quantifying peat bulk density, organic matter and carbon content for  
579 palaeostudies of climate and peatland carbon dynamics. *Mires Peat* 7, 1–10.

580 Chapman, S.J., Bell, J., Donnelly, D., Lilly, A., 2009. Carbon stocks in Scottish peatlands.  
581 *Soil Use Manag.* 25, 105–112. <https://doi.org/10.1111/j.1475-2743.2009.00219.x>

582 Charman, D.J., 2002. Peatlands and environmental change, Peatlands and environmental  
583 change. John Wiley & Sons Ltd.

584 Charman, D.J., Beilman, D.W., Blaauw, M., Booth, R.K., Brewer, S., Chambers, F.M.,  
585 Christen, J.A., Gallego-Sala, A., Harrison, S.P., Hughes, P.D.M., Jackson, S.T.,  
586 Korhola, A., Mauquoy, D., Mitchell, F.J.G., Prentice, I.C., Van Der Linden, M., De  
587 Vleeschouwer, F., Yu, Z.C., Alm, J., Bauer, I.E., Corish, Y.M.C., Garneau, M., Hohl,  
588 V., Huang, Y., Karofeld, E., Le Roux, G., Loisel, J., Moschen, R., Nichols, J.E.,  
589 Nieminen, T.M., MacDonald, G.M., Phadtare, N.R., Rausch, N., Sillasoo, U., Swindles,  
590 G.T., Tuittila, E.S., Ukonmaanaho, L., Valiranta, M., Van Bellen, S., Van Geel, B., Vitt,  
591 D.H., Zhao, Y., 2013. Climate-related changes in peatland carbon accumulation during  
592 the last millennium. *Biogeosciences* 10, 929–944. [https://doi.org/10.5194/bg-10-929-](https://doi.org/10.5194/bg-10-929-2013)  
593 2013

594 Comas, X., Slater, L., Reeve, A., 2005. Stratigraphic controls on pool formation in a domed  
595 bog inferred from ground penetrating radar (GPR). *J. Hydrol.* 315, 40–51.

596 <https://doi.org/10.1016/J.JHYDROL.2005.04.020>

597 Cruickshank, M., Tomlinson, R., Devine, P., Milne, R., 1998. Carbon in the vegetation and  
598 soils of Northern Ireland. *Biol. Environ.* 98.

599 Dallaire, P.-L., Garneau, M., 2008. The use of a ground-penetrating radar (GPR) to  
600 characterize peat stratigraphy and estimate the carbon pool in a boreal peatland,  
601 Eastmain region, James Bay, Québec, Canada. *12th Int. Conf. Gr. Penetrating Radar.*

602 Doolittle, J., Butnor, J., 2009. Soils, peatlands, and biomonitoring, in: *Ground Penetrating*  
603 *Radar.* Elsevier, pp. 177–202. <https://doi.org/10.1016/B978-0-444-53348-7.00006-5>

604 Environment Agency, 2013. Geomatics Group. Rivers House, Lower Bristol Road, Bath.  
605 [https://doi.org/https://environment.maps.arcgis.com/apps/MapJournal/index.html?appid](https://doi.org/https://environment.maps.arcgis.com/apps/MapJournal/index.html?appid=c6cef6cc642a48838d38e722ea8ccfee#)  
606 [=c6cef6cc642a48838d38e722ea8ccfee#](https://doi.org/https://environment.maps.arcgis.com/apps/MapJournal/index.html?appid=c6cef6cc642a48838d38e722ea8ccfee#)

607 European Commission. 2007. *Interpretation Manual of European Union Habitats, 2007.*

608 Evans, C., Artz, R., Moxley, J., Smyth, M.-A., Taylor, E., Archer, N., Burden, A.,  
609 Williamson, J., Donnelly, D., Thomson, A., Buys, G., Malcolm, H., Wilson, D., Renou-  
610 Wilson, F., Potts, J., Chris Evans, P., 2017. *Implementation of an Emissions Inventory*  
611 *for UK Peatlands. Report to the Department for Business, Energy & Industrial Strategy.*

612 Evans, C., Morrison, R., Burden, A., Williamson, J., Baird, A., Brown, E., Callaghan, N.,  
613 Chapman, P., Cumming, A., Dean, H., Dixon, S., Dooling, G., Evans, J., Gauci, V.,  
614 Grayson, R., Haddaway, N., He, Y., Heppel, K., Holden, J., Hughes, S., Kaduk, J.,  
615 Jones, D., Matthews, R., Menichino, N., Misselbrook, T., Page, S., Pan, G., Peacock,  
616 M., Rayment, M., Ridley, L., Robinson, I., Rylett, D., Scowen, M., Stanley, K., Worrall,  
617 F., 2016. *Lowland peat systems in England and Wales - evaluating greenhouse gas*  
618 *fluxes and carbon balances (DEFRA Project SP1210).*

619 Francke, J., 2012. A review of selected ground penetrating radar applications to mineral  
620 resource evaluations. *J. Appl. Geophys.* 81, 29–37.  
621 <https://doi.org/10.1016/j.jappgeo.2011.09.020>

622 Fyfe, R.M., Coombe, R., Davies, H., Parry, L., 2014. The importance of sub-peat carbon  
623 storage as shown by data from Dartmoor, UK. *Soil Use Manag.* 30, 23–31.  
624 <https://doi.org/10.1111/sum.12091>

625 Gallego-Sala, A. V., Clark, J.M., House, J.I., Orr, H.G., Prentice, I.C., Smith, P., Farewell, T.,  
626 Chapman, S.J., 2010. Bioclimatic envelope model of climate change impacts on blanket  
627 peatland distribution in Great Britain. *Clim. Res.* 45, 151–162.  
628 <https://doi.org/10.3354/cr00911>

629 Gallego-Sala, A. V, Charman, D.J., Brewer, S., Page, S.E., Prentice, I.C., Friedlingstein, P.,  
630 Moreton, S., Amesbury, M.J., Beilman, D.W., Björck, S., Blyakharchuk, T., Bohicchio,  
631 C., Booth, R.K., Bunbury, J., Camill, P., Carless, D., Chimner, R.A., Clifford, M.,  
632 Cressey, E., Courtney-Mustaphi, C., De Vleeschouwer, F., De Jong, R., Fialkiewicz-  
633 Koziel, B., Finkelstein, S.A., Garneau, M., Githumbi, E., Hribljan, J., Holmquist, J.,  
634 Hughes, P.D.M., Jones, C., Jones, M.C., Karofeld, E., Klein, E.S., Kokfelt, U., Korhola,  
635 A., Lacourse, T., Le Roux, G., Lamentowicz, M., Large, D., Lavoie, M., Loisel, J.,  
636 Mackay, H., Macdonald, G.M., Makila, M., Magnan, G., Marchant, R., Marcisz, K.,  
637 Cortizas, A.M., Massa, C., Mathijssen, P., Mauquoy, D., Mighall, T., Mitchell, F.J.G.,  
638 Moss, P., Nichols, J., Oksanen, P.O., Orme, L., Packalen, M.S., Robinson, S., Roland,  
639 T.P., Sanderson, N.K., Britta, A., Sannel, K., Silva-Sánchez, N., Steinberg, N.,  
640 Swindles, G.T., Turner, T.E., Uglow, J., Väliranta, M., Van Bellen, S., Van Der Linden,  
641 M., Van Geel, B., Wang, G., Yu, Z., Zaragoza-Castells, J., Zhao, Y., n.d. Latitudinal  
642 limits to the predicted increase of the peatland carbon sink with warming  
643 SUPPLEMENTARY INFORMATION. <https://doi.org/10.1038/s41558-018-0271-1>

644 Gatis, N., Luscombe, D.J., Carless, D., Parry, L.E., Fyfe, R.M.M., Harrod, T.R., Brazier,  
645 R.E., Anderson, K., 2019. Mapping upland peat depth using airborne radiometric and  
646 lidar survey data. *Geoderma* 335, 78–87.  
647 <https://doi.org/10.1016/j.geoderma.2018.07.041>

648 George, D., 1990. *The Brecon Beacons National Park its Climate and Mountain Weather*,  
649 Cardiff Weather Centre Information Booklet. Met Office. [https://doi.org/ISBN 0-86180-](https://doi.org/ISBN%200-86180-281-0)  
650 281- 0.

651 Goovaerts, P., 1997. *Geostatistics for Natural Resources Evaluation*, in: *Mathematical*  
652 *Geology*. Department of Civil and Environmental Engineering, The University of  
653 Michigan.

654 Gorham, E., 1991. Northern Peatlands : Role in the Carbon Cycle and Probable Responses to  
655 Climatic Warming. *Ecol. Appl.* 1, 182–195.

656 Grand-Clement, E., Anderson, K., Smith, D., Luscombe, D., Gatis, N., Ross, M., Brazier,  
657 R.E., 2013. Evaluating ecosystem goods and services after restoration of marginal  
658 upland peatlands in South-West England. *J. Appl. Ecol.* 50, 324–334.  
659 <https://doi.org/10.1111/1365-2664.12039>

660 Gusmeroli, A., Jansson, P., Pettersson, R., Murray, T., 2012. Twenty years of cold surface  
661 layer thinning at Storglaciären, sub-Arctic Sweden, 1989-2009. *J. Glaciol.*  
662 <https://doi.org/10.3189/2012JoG11J018>

663 Hänninen, P., 1992. Geological Survey of Finland, Bulletin 361 Application of ground  
664 penetrating radar and radio wave moisture probe techniques to peatland investigations.

665 Holden, J., Burt, T.P., Vilas, M., 2002. Application of ground-penetrating radar to the  
666 identification of subsurface piping in blanket peat. *Earth Surf. Process. Landforms* 27,  
667 235–249. <https://doi.org/10.1002/esp.316>



668 Holden, N.M., Connolly, J., 2011. Estimating the carbon stock of a blanket peat region using  
669 a peat depth inference model. *Catena* 86, 75–85.  
670 <https://doi.org/10.1016/j.catena.2011.02.002>

671 Howie, S.A., Meerveld, I.T. Van, 2011. The essential role of the lagg in raised bog function  
672 and restoration: A review. *Wetlands* 31, 613–622. [https://doi.org/10.1007/s13157-011-](https://doi.org/10.1007/s13157-011-0168-5)  
673 [0168-5](https://doi.org/10.1007/s13157-011-0168-5)

674 Huisman, J.A., Hubbard, S.S., Redman, J.D., Annan, A.P., 2003. Measuring soil water  
675 content with ground penetrating radar: A review. *Vadose Zo. J.* 2, 476–491.  
676 <https://doi.org/10.2113/2.4.476>

677

678

679

680 IUCN, 2017. IUCN Issue Brief: Peatlands and Climate Change. IUCN.Org.

681 Jol, H.M., Smith, D.G., 1995. Ground penetrating radar surveys of peatlands for oilfield  
682 pipelines in Canada. *J. Appl. Geophys.* 34, 109–123. [https://doi.org/10.1016/0926-](https://doi.org/10.1016/0926-9851(95)00018-6)  
683 [9851\(95\)00018-6](https://doi.org/10.1016/0926-9851(95)00018-6)

684 Joosten, H., Clarke, D., 2002. *Wise Use of Mires and Peatlands - Background and Principles*  
685 *Including Framework for Decision-Making.*

686 Joosten, H., Tapio-Biström, M.-L., Tol, S., 2012. *Peatlands - guidance for climate change:*  
687 *mitigation through conservation, rehabilitation and sustainable use, Mitigation of*  
688 *Climate Change in Agriculture (MICCA) Programme series 5.*

689 Lal, R., 2008. Sequestration of atmospheric CO<sub>2</sub> in global carbon pools. *Energy Environ. Sci.*  
690 1, 86. <https://doi.org/10.1039/b809492f>

691 Limpens, J., Berendse, F., Blodau, C., Canadell, J.G., Freeman, C., Holden, J., Roulet, N.,  
692 Rydin, H., Schaepman-Strub, G., 2008. Peatlands and the carbon cycle: from local  
693 processes to global implications-a synthesis, *Biogeosciences*.

694 Lindsay, R., 2010. Peatbogs and Carbon. A critical synthesis to inform policy development in  
695 oceanic peat bog conservation and restoration in the context of climate change. RSPB.

696 Lindsay, R., Birnie, R., Clough, J., 2014. IUCN UK Committee Peatland Programme,  
697 Briefing Note 7, Grazing and trampling, IUCN UK Committee Peatland Programme.

698 Loisel, J., Yu, Z., Beilman, D.W., Camill, P., Alm, J., Amesbury, M.J., Anderson, D.,  
699 Andersson, S., Bochicchio, C., Barber, K., Belyea, L.R., Bunbury, J., Chambers, F.M.,  
700 Charman, D.J., De Vleeschouwer, F., Fiałkiewicz-Kozieł, B., Finkelstein, S.A., Gałka,  
701 M., Garneau, M., Hammarlund, D., Hinchcliffe, W., Holmquist, J., Hughes, P., Jones,  
702 M.C., Klein, E.S., Kokfelt, U., Korhola, A., Kuhry, P., Lamarre, A., Lamentowicz, M.,  
703 Large, D., Lavoie, M., MacDonald, G., Magnost, G., Mäkilä, M., Mallon, G.,  
704 Mathijssen, P., Mauquoy, D., McCarroll, J., Moore, T.R., Nichols, J., O'Reilly, B.,  
705 Oksanen, P., Packalen, M., Peteet, D., Richard, P.J., Robinson, S., Ronkainen, T.,  
706 Rundgren, M., Sannel, A.B.K., Tarnocai, C., Thom, T., Tuittila, E.-S., Turetsky, M.,  
707 Väiliranta, M., van der Linden, M., van Geel, B., van Bellen, S., Vitt, D., Zhao, Y., Zhou,  
708 W., 2014. A database and synthesis of northern peatland soil properties and Holocene  
709 carbon and nitrogen accumulation. *The Holocene* 24, 1028–1042.  
710 <https://doi.org/10.1177/0959683614538073>

711 McClellan, M., Comas, X., Benscoter, B., Hinkle, R., Sumner, D., 2017. Estimating  
712 Belowground Carbon Stocks in Isolated Wetlands of the Northern Everglades  
713 Watershed, Central Florida, Using Ground Penetrating Radar and Aerial Imagery. *J.*  
714 *Geophys. Res. Biogeosciences* 122, 2804–2816. <https://doi.org/10.1002/2016JG003573>

715 Milne, R., Brown, T.A., 1997. Carbon in the Vegetation and Soils of Great Britain, *Journal of*  
716 *Environmental Management*.

717 Ostle, N.J., Levy, P.E., Evans, C.D., Smith, P., 2009. UK land use and soil carbon  
718 sequestration. *Land use policy*. <https://doi.org/10.1016/j.landusepol.2009.08.006>

719 Parry, L.E., Charman, D.J., Noades, J.P.W., 2012. A method for modelling peat depth in  
720 blanket peatlands. *Soil Use Manag.* 28, 614–624. [https://doi.org/10.1111/j.1475-](https://doi.org/10.1111/j.1475-2743.2012.00447.x)  
721 [2743.2012.00447.x](https://doi.org/10.1111/j.1475-2743.2012.00447.x)

722 Parry, L.E., West, L.J., Holden, J., Chapman, P.J., 2014. Evaluating approaches for  
723 estimating peat depth. *J. Geophys. Res. Biogeosciences* 119, 567–576.  
724 <https://doi.org/10.1002/2013JG002411>

725 Parsekian, A.D., Slater, L., Ntarlagiannis, D., Nolan, J., Sebesteyen, S.D., Kolka, R.K.,  
726 Hanson, P.J., 2012. Uncertainty in Peat Volume and Soil Carbon Estimated Using  
727 Ground-Penetrating Radar and Probing. *Soil Sci. Soc. Am. J.* 76, 1911.  
728 <https://doi.org/10.2136/sssaj2012.0040>

729 Petrokofsky, G., Kanamaru, H., Achard, F., Goetz, S.J., Joosten, H., Holmgren, P., Lehtonen,  
730 A., Menton, M.C., Pullin, A.S., Wattenbach, M., 2012. Comparison of methods for  
731 measuring and assessing carbon stocks and carbon stock changes in terrestrial carbon  
732 pools. How do the accuracy and precision of current methods compare? A systematic  
733 review protocol. *Environ. Evid.* 1, 6. <https://doi.org/10.1186/2047-2382-1-6>

734 Plado, J., Sibul, I., Mustasaar, M., Jõelett, A., 2011. Ground-penetrating radar study of the  
735 Rahivere peat bog, eastern Estonia. *Est. J. Earth Sci.* 60, 31–42.  
736 <https://doi.org/10.3176/earth.2011.1.03>

737 Pratt-Heaton, C., 1999. Visitors and Visitor Pressure in the Brecon Beacons National Park  
738 SCOPE: Tourism and effects of pressure from tourism.

- 739 Price, M., 2002. Deriving Volumes With ArcGIS. *ArcUser* 52–56.  
740 <https://doi.org/10.1177/004728758502400106>
- 741 Proulx-McInnis, S., St-Hilaire, A., Rousseau, A.N., Jutras, S., 2013. A review of ground-  
742 penetrating radar studies related to peatland stratigraphy with a case study on the  
743 determination of peat thickness in a northern boreal fen in Quebec, Canada. *Prog. Phys. Geogr.* <https://doi.org/10.1177/0309133313501106>
- 745 Rosa, E., Larocque, M., Pellerin, S., Gagné, S., Fournier, B., 2009. Determining the number  
746 of manual measurements required to improve peat thickness estimations by ground  
747 penetrating radar. *Earth Surf. Process. Landforms* 34, 377–383.  
748 <https://doi.org/10.1002/esp.1741>
- 749 Ryazantsev, P., Mironov, V., 2018. Study of peatland internal structure by the Ground  
750 Penetrating Radar, in: 2018 17th International Conference on Ground Penetrating Radar,  
751 GPR 2018. Institute of Electrical and Electronics Engineers Inc.  
752 <https://doi.org/10.1109/ICGPR.2018.8441680>
- 753 Sandeimer, K., 2013. Reflex-Win version 7.0.3.
- 754 Sass, O., Friedmann, A., Haselwanter, G., Wetzel, K.F., 2010. Investigating thickness and  
755 internal structure of alpine mires using conventional and geophysical techniques. *Catena*  
756 80, 195–203. <https://doi.org/10.1016/j.catena.2009.11.006>
- 757 Smith, P., Smith, J., Flynn, H., Killham, K., Rangel-Castro, Ignacio Foereid, B., Aitkenhead,  
758 M., Chapman, S., Towers, W., Bell, J., Lumsdon, D., Milne, R., Thomson, A.,  
759 Simmons, I., Skiba, U., Reynolds, B., Evans, C., Frogbrook, Z., Bradley, I., Whitmore,  
760 A., Falloon, P., 2007. Estimating carbon in organic soils sequestration and emission,  
761 ECOSSE.
- 762 Theimer, B.D., Nobes, D.C., Warner, B.G., 1994. A study of the geoelectrical properties of

763 peatlands and their influence on ground-penetrating radar surveying. *Geophys. Prospect.*  
764 42, 179–209.

765 Ulriksen, C.P., 1982. *Application of Impulse Radar to civil engineering: [Thesis].* Lund  
766 University of Technology.

767 Warner, B.G., Nobes, D.C., Theimer, B.D., 1990. An application of ground penetrating radar  
768 to peat stratigraphy of Ellice Swamp, southwestern Ontario. *Can. J. Earth Sci.* 27, 932–  
769 938. <https://doi.org/10.1139/e90-096>

770 Wellock, M.L., Reidy, B., Laperle, C.M., Bolger, T., Kiely, G., 2011. Soil organic carbon  
771 stocks of afforested peatlands in Ireland. *Forestry* 84, 441–451.  
772 <https://doi.org/10.1093/forestry/cpr046>

773 Welsh Government, 2019a. *Prosperity for all: A climate conscious Wales. A climate change*  
774 *adaptation plan for Wales.*

775 Welsh Government, 2019b. *Achieving our low carbon pathway to 2030. Welsh Government*  
776 *Response.*

777 Welsh Government, 2019c. *Decision reports: 2019 [WWW Document].* URL  
778 <https://gov.wales/decision-reports-2019> (accessed 1.24.21).

779 Worsfold, R.D., Parashar, S.K., Perrott, T., 1986. Depth profiling of peat deposits with  
780 impulse radar. *Can. Geotech. J.* 23, 142–154. <https://doi.org/10.1139/t86-024>

781 Yu, Z., Beilman, D.W., Frohking, S., MacDonald, G.M., Roulet, N.T., Camill, P., Charman,  
782 D.J., 2011. Peatlands and Their Role in the Global Carbon Cycle. *Eos, Trans. Am.*  
783 *Geophys. Union* 92, 97. <https://doi.org/10.1029/2011EO120001>

784 Yu, Z.C., 2012. Northern peatland carbon stocks and dynamics: a review. *Biogeosciences* 9,  
785 4071–4085. <https://doi.org/10.5194/bg-9-4071-2012>

786 Zeng, H., Huang, S., 2007. Research on spatial data interpolation based on Kriging  
787 interpolation. Eng. Surv. Mapp. 16, 5–8.

788